Supplementary information

A giant Nernst power factor and figure-of-merit in polycrystalline $NbSb_2$ for Ettingshausen refrigeration

Peng Li[a,b], Pengfei Qiu[a,b,c]*, Jie Xiao[a], Tingting Deng[c], Lidong Chen[a,b], and Xun Shi[a,b]*

[a]State Key Laboratory of High Performance Ceramics and Superfine Microstructure, Shanghai Institute of Ceramics, Chinese Academy of Science, Shanghai 200050, China

[b]Center of Materials Science and Optoelectronics Engineering, University of Chinese Academy of Sciences, Beijing 100049, China

[c]School of Chemistry and Materials Science, Hangzhou Institute for Advanced Study, University of Chinese Academy of Sciences, Hangzhou 310024, China

*Email: *qiupf@mail.sic.ac.cn; xshi@mail.sic.ac.cn*

Supplementary Note 1

Separation of the diffusion component ($S_d^h - S_d^e$) and phonon-drag component ($S_p^h - S_p^e$) from the measured Seebeck thermopower.

Due to the large overlap (350 meV) of the conduction and valence bands[1], $NbSb_2$ can be viewed as a strong degenerate system, where the diffusion component of Seebeck thermopower of electrons and holes varies linearly with temperature[2]. Therefore, the phonon-drag component ($S_p^h - S_p^e$) can be obtained by subtracting the linear extrapolation of diffusion component ($S_d^h - S_d^e$) from the total Seebeck thermopower difference $(S_{xx}^h - S_{xx}^e)$[3]. As shown in Figure 4f, for single-crystalline and polycrystalline $NbSb_2$, ($S_d^h - S_d^e$) dominates above 80 K, and ($S_p^h - S_p^e$) dominates over the ($S_d^h - S_d^e$) below 80 K.

Supplementary Note 2

Derivation process of Nernst figure-of-merit z_N

Figure S1 shows the schematics of a rectangular Ettingshausen refrigerator, with the dimensions along the temperature difference direction, the current direction, and the applied magnetic field direction as L_x, L_y, and L_z, respectively. The temperature gradient in the x-direction is $\nabla_x T$. The electric field strength in the y-direction is ϵ_y. In unit time, the amount of heat extracted by the Ettinghausen effect is $S_{yx}T_l\epsilon_y\sigma_{yy}L_yL_z$, where S_{yx} is the Nernst thermopower, T_l is the temperature of the cold end, and σ_{yy} is the electrical conductivity along the y-axis. The Joule heat flowing into the cold end is $\frac{1}{2}\epsilon_y^2\sigma_{yy}L_xL_yL_z$ and the heat of conduction from the hot end to the cold end is $\kappa_{xx}\nabla_x TL_yL_z$, where κ_{xx} is the thermal conductivity along the x-axis. The refrigeration capacity of the cold end per unit of time Q_{in} is

$$Q_{in} = \left[S_{yx}T_l\epsilon_y\sigma_{yy} - \frac{1}{2}\epsilon_y^2\sigma_{yy}L_x - \kappa_{xx}\nabla_x T\right]L_yL_z \quad 1 \tag{S1}$$

The input power P of the Ettingshausen refrigerator is

$$P = \left(\epsilon_y^2\sigma_{yy} + S_{yx}\nabla_x T\epsilon_y\sigma_{yy}\right)L_xL_yL_z \tag{S2}$$

The COP of the Ettingshausen refrigerator is

$$COP = \frac{Q_{in}}{P} = \frac{S_{yx}T_l\epsilon_y\sigma_{yy} - \frac{1}{2}\epsilon_y^2\sigma_{yy}L_x - \kappa_{xx}\nabla_x T}{\left(\epsilon_y^2\sigma_{yy} + S_{yx}\nabla_x T\epsilon_y\sigma_{yy}\right)L_x} \tag{S3}$$

According to dCOP/$d\epsilon_y$= 0, the optimum electric field strength is

$$\epsilon_{y,COP} = S_{yx}\nabla_x T\frac{1}{\sqrt{1+z_N\overline{T}}-1} \tag{S4}$$

In this case, the maximum COP can be obtained as

$$COP_{max} = \frac{T_l}{T_h - T_l}\frac{\sqrt{1+z_N\overline{T}} - \frac{T_h}{T_l}}{\sqrt{1+z_N\overline{T}}+1} \tag{S5}$$

where z_N is $\frac{S_{yx}^2\sigma_{yy}}{\kappa_{xx}}$ and $\overline{T}$ is the average temperature of hot end and cold end $\frac{1}{2}(T_h + T_l)$. Thus, the z_N is a parameter that independent on the material's geometric factors.

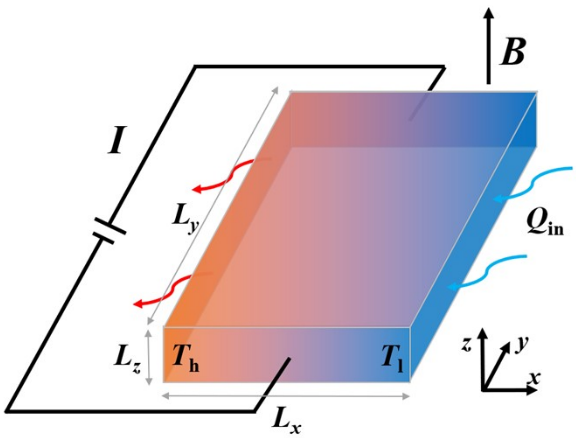

Figure S1 Schematics of a rectangular Ettingshausen refrigerator.

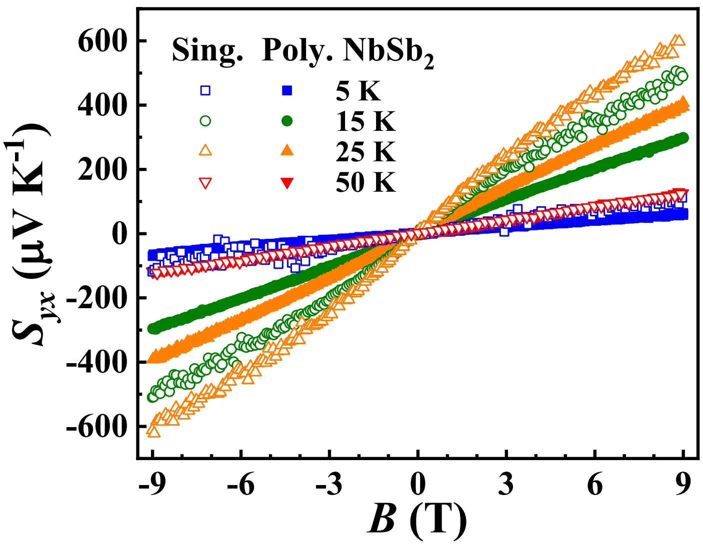

Figure S2 Magnetic field dependences of Nernst thermopower S_{yx} of polycrystalline $NbSb_2$ at different temperatures. The data of single-crystalline $NbSb_2$ are included for comparison[1].

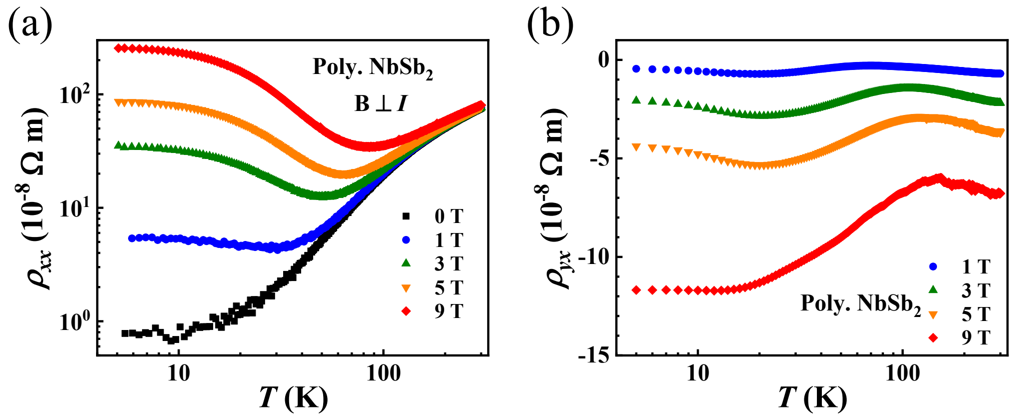

Figure S3 Temperature dependence of (a) electrical resistivity ρ_{xx} and (b) Hall resistivity ρ_{yx} for polycrystalline $NbSb_2$ under different magnetic fields.

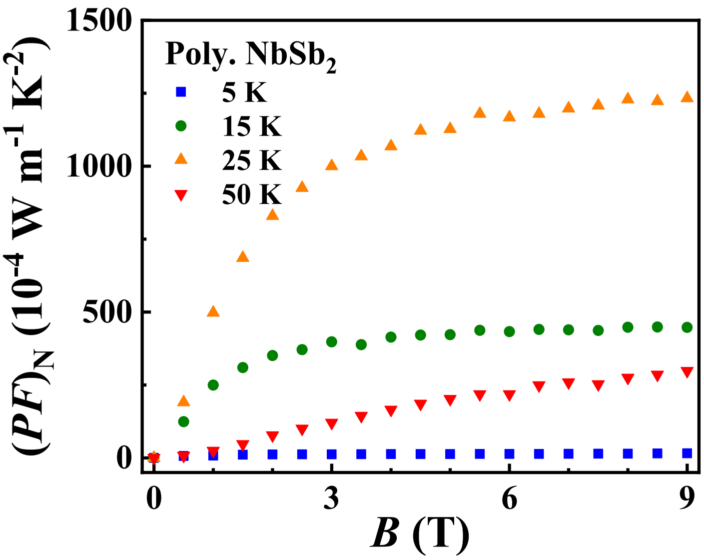

Figure S4 Magnetic field dependence of Nernst power factor $(PF)_N$ for polycrystalline $NbSb_2$ at different temperatures.

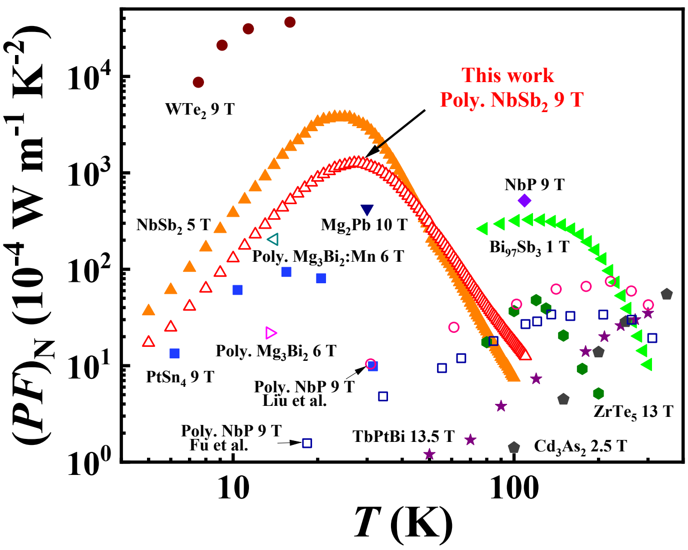

Figure S5 Temperature dependences of $(PF)_N$ typical polycrystalline thermomagnetic materials under different magnetic fields. The data are taken from References 1, 4-16. The hollow symbols are for polycrystals, while the solid symbols are for single crystals.

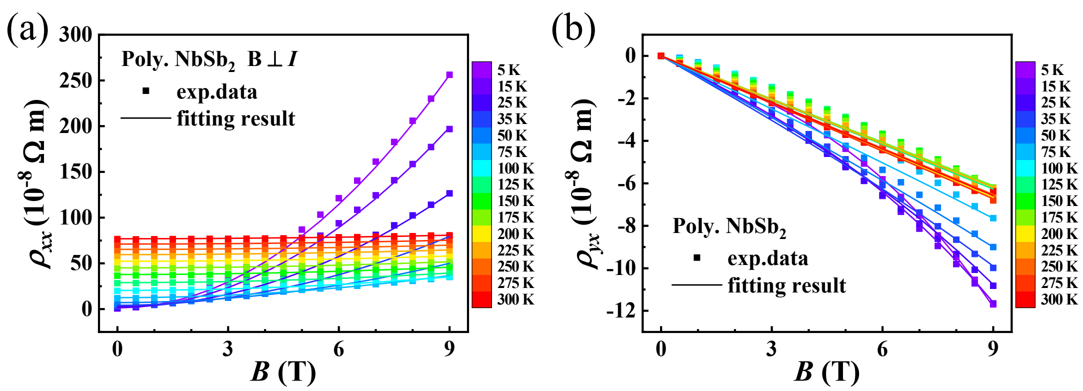

Figure S6 Fitting of the (a) electrical resistivity $\rho_{xx}(B)$ and (b) Hall resistivity $\rho_{yx}(B)$ for polycrystalline $NbSb_2$ under different temperatures. The symbols are experimental data and the lines are the fitting curves.

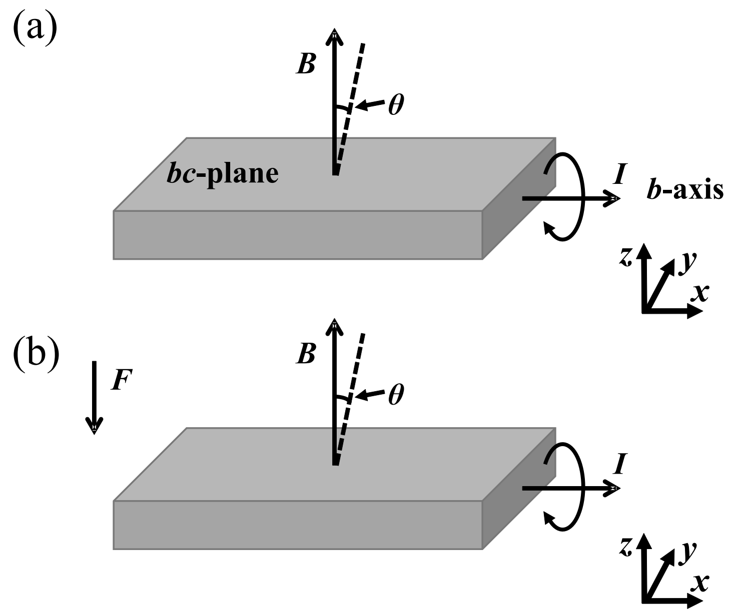

Figure S7 Schematic diagram of the angle dependence of electrical resistivity ρ measurement for (a) single-crystalline $NbSb_2$ and (b) polycrystalline $NbSb_2$. ***F*** represent the direction of the sintering pressure of polycrystalline $NbSb_2$.

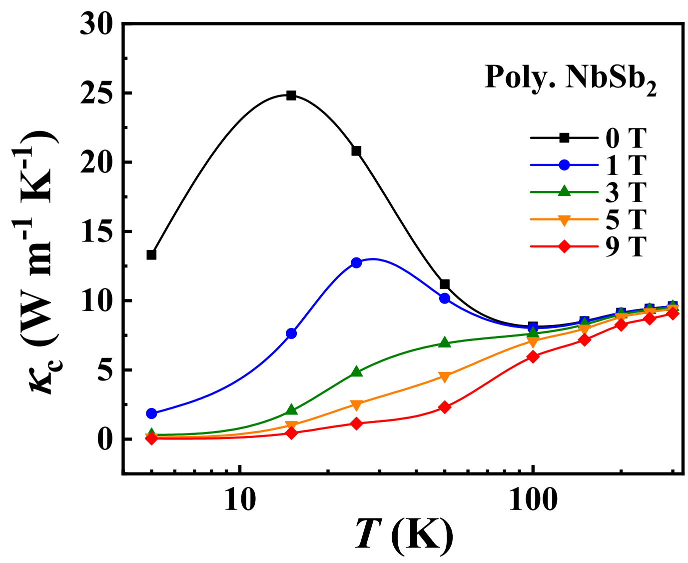

Figure S8 Temperature dependence of the carrier thermal conductivity κ_c for polycrystalline $NbSb_2$ at different magnetic fields obtained from the empirical equation.

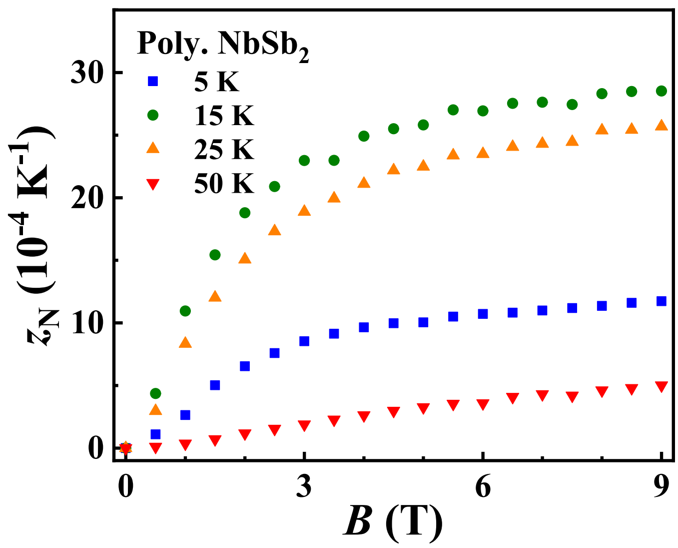

Figure S9 Magnetic field dependence of Nernst figure-of-merit z_N for polycrystalline $NbSb_2$ at different temperatures.

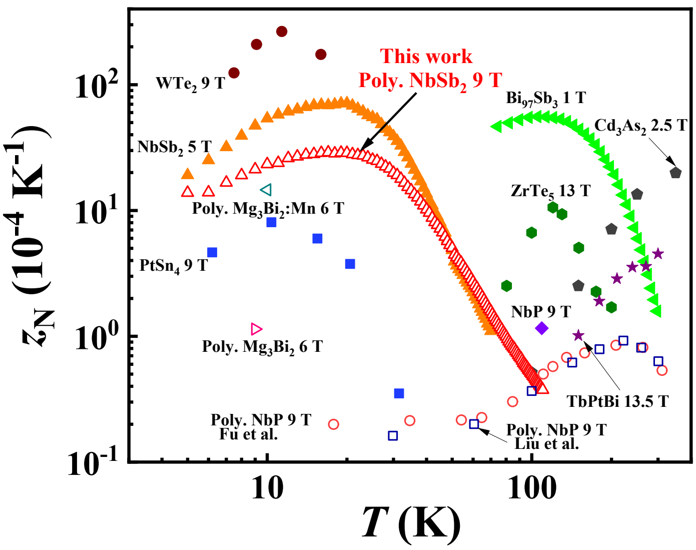

Figure S10 Temperature dependences of Nernst figure-of-merit z_N of typical polycrystalline thermomagnetic materials under different magnetic fields. The data are taken from References 1, 5-16. The hollow symbols are for polycrystals, while the solid symbols are for single crystals.

Table S1 Parameters used to fit the measured thermal conductivity of polycrystalline $NbSb_2$.

T (K)	κ_l (W m^{-1} K^{-1})	κ_c (0,T) (W m^{-1} K^{-1})	$\eta^{1/s}$ (T $^{-1}$)	s
5	1.18	13.30	2.83	1.75
15	15.15	24.81	1.75	1.45
25	47.59	20.81	0.74	1.51
50	57.12	11.19	0.25	1.66
100	29.31	8.13	0.058	1.55
150	20.08	8.52	0.042	1.72
200	15.95	9.13	0.033	1.85
250	14.22	9.42	0.030	1.91
300	13.72	9.61	0.025	1.89

Supplementary references

1. P. Li, P. Qiu, Q. Xu, J. Luo, Y. Xiong, J. Xiao, N. Aryal, Q. Li, L. Chen and X. Shi, *Nat. Commun.*, 2022, **13**, 7612.
2. F. J. Blatt, P. A. Schroeder, C. L. Foiles and D. Greig, *Thermoelectric power of metals*, Plenum Press, New York and London, 1976.
3. V. D. Kagan, N. A. Red'ko, N. A. Rodionov, V. I. Pol'shin and O. V. Zotova, *Physics of the Solid State*, 2004, **46**, 1410-1419.
4. Z. Chen, X. Zhang, J. Ren, Z. Zeng, Y. Chen, J. He, L. Chen and Y. Pei, *Nat. Commun.*, 2021, **12**, 3837.
5. C. Fu, S. N. Guin, T. Scaffidi, Y. Sun, R. Saha, S. J. Watzman, A. K. Srivastava, G. Li, W. Schnelle, S. S. P. Parkin, C. Felser and J. Gooth, *Research*, 2020, **2020**, 4643507.
6. Y. Pan, B. He, T. Helm, D. Chen, W. Schnelle and C. Felser, *Nat. Commun.*, 2022, **13**, 3909.
7. K. F. Cuff, R. B. Horst, J. L. Weaver, S. R. Hawkins, C. F. Kooi and G. M. Enslow, *Appl. Phys. Lett.*, 1963, **2**, 145-146.
8. P. Wang, C. Cho, F. Tang, P. Wang, W. Zhang, M. He, G. Gu, X. Wu, Y. Shao and L. Zhang, *Phys. Rev. B*, 2021, **103**, 045203.
9. S. J. Watzman, T. M. McCormick, C. Shekhar, S.-C. Wu, Y. Sun, A. Prakash, C. Felser, N. Trivedi and J. P. Heremans, *Phys. Rev. B*, 2018, **97**, 161404(R).
10. C. Shekhar, A. K. Nayak, Y. Sun, M. Schmidt, M. Nicklas, I. Leermakers, U. Zeitler, Y. Skourski, J. Wosnitza, Z. Liu, Y. Chen, W. Schnelle, H. Borrmann, Y. Grin, C. Felser and B. Yan, *Nat. Phys.*, 2015, **11**, 645-649.
11. J. Xiang, S. Hu, M. Lyu, W. Zhu, C. Ma, Z. Chen, F. Steglich, G. Chen and P. Sun, *Sci. China: Phys., Mech. Astron.*, 2019, **63**, 237011.
12. H. Wang, Z. Zhou, J. Ying, Z. Xiang, R. Wang, A. Wang, Y. Chai, M. He, X. Lu, G. Han, Y. Pan, G. Wang, X. Zhou and X. Chen, *Adv. Mater.*, 2023, **35**, 2206941.
13. T. Feng, P. Wang, Z. Han, L. Zhou, W. Zhang, Q. Liu and W. Liu, *Adv. Mater.*, 2022, **34**, 2200931.
14. T. Feng, P. Wang, Z. Han, L. Zhou, Z. Wang, W. Zhang, Q. Liu and W. Liu, *Energy Environ. Sci.*, 2023, **16**, 1560-1568.
15. C. Fu, S. N. Guin, S. J. Watzman, G. Li, E. Liu, N. Kumar, V. Süβ, W. Schnelle, G. Auffermann, C. Shekhar, Y. Sun, J. Gooth and C. Felser, *Energy Environ. Sci.*, 2018, **11**, 2813-2820.
16. W. Liu, Z. Wang, J. Wang, H. Bai, Z. Li, J. Sun, X. Zhou, J. Luo, W. Wang, C. Zhang, J. Wu, Y. Sun, Z. Zhu, Q. Zhang and X. Tang, *Adv. Funct. Mater.*, 2022, **32**, 2202143.